Electronic Supplementary Material (ESI) for Journal of Materials Chemistry A.

Supporting Information

Ultrafast Charge/Discharge Solid-State Thin-Film Supercapacitor via Regulating the Microstructure of Transition-Metal-Oxide

Qiying Lv[a‡], Kai Chi[a‡], Yan Zhang[a], Fei Xiao[a], Junwu Xiao[a], Shuai Wang[*a, b], Kian Ping Loh[c]

[1]School of Chemistry & Chemical Engineering, Huazhong University of Science and Technology,Wuhan 430074, P. R. China

[2]State Key Laboratory of Digital Manufacturing Equipment and Technology, Flexible Electronics Research Center (FERC), School of Mechanical Science and Engineering, Huazhong University of Science and Technology, Wuhan 430074, P.R. China

[3]Department of Chemistry, National University of Singapore, 3 Science Drive 3, Singapore 117543

[‡]These authors contributed equally to this work.

*Email: chmsamuel@mail.hust.edu.cn

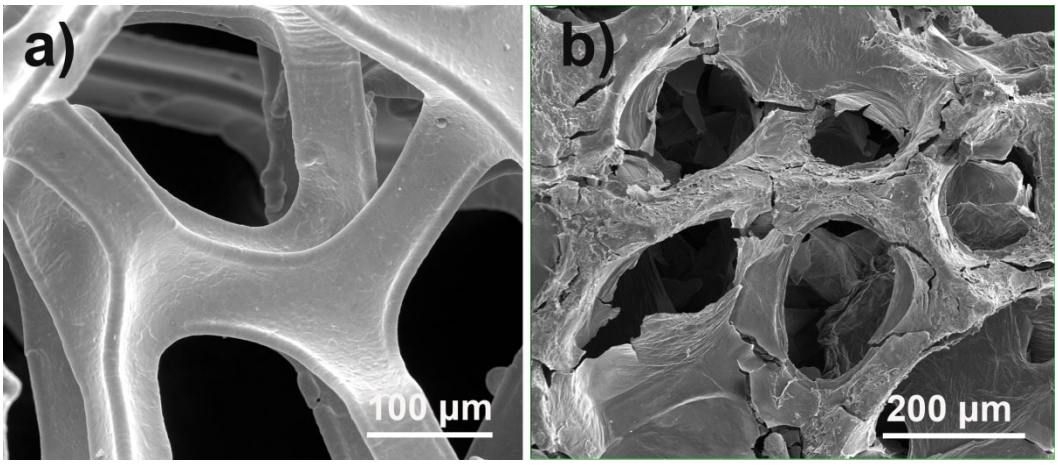

Fig. S1 FESEM images of NF (**a**) and NF/rGO (**b**) electrodes, respectively.

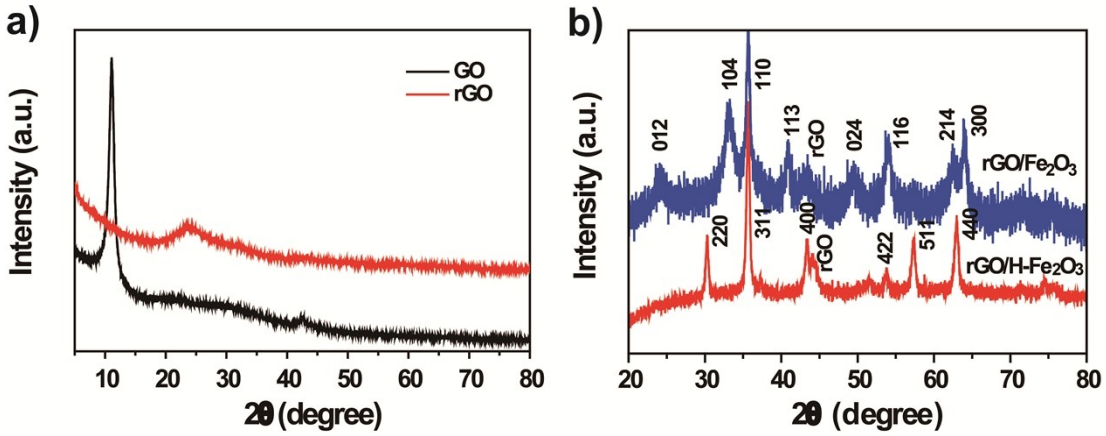

Fig. S2 X-ray diffraction patterns of the samples. **a**) X-ray diffraction patterns of GO, rGO; **b**) X-ray diffraction patterns of rGO/H-Fe_2O_3, rGO/Fe_2O_3.

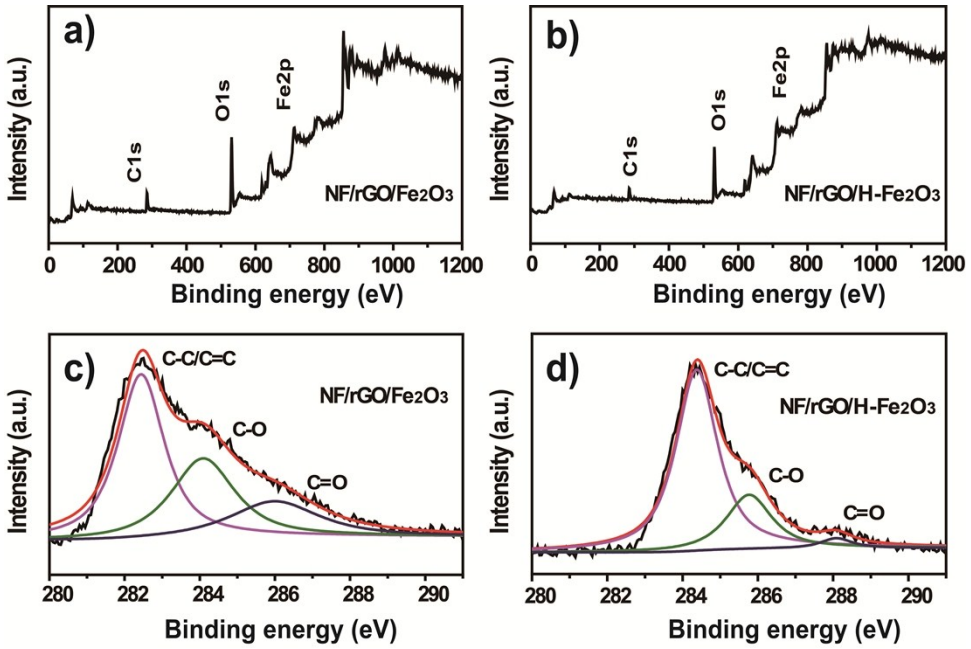

Fig. S3 The survey spectra for the NF/rGO/Fe_2O_3 (**a**) and NF/rGO/H-Fe_2O_3 (**b**) samples, respectively; **c**) High-resolution XPS spectra of C 1s of the NF/rGO/Fe_2O_3 sample; **d**) High-resolution XPS spectra of C 1s of the NF/rGO/H-Fe_2O_3 sample.

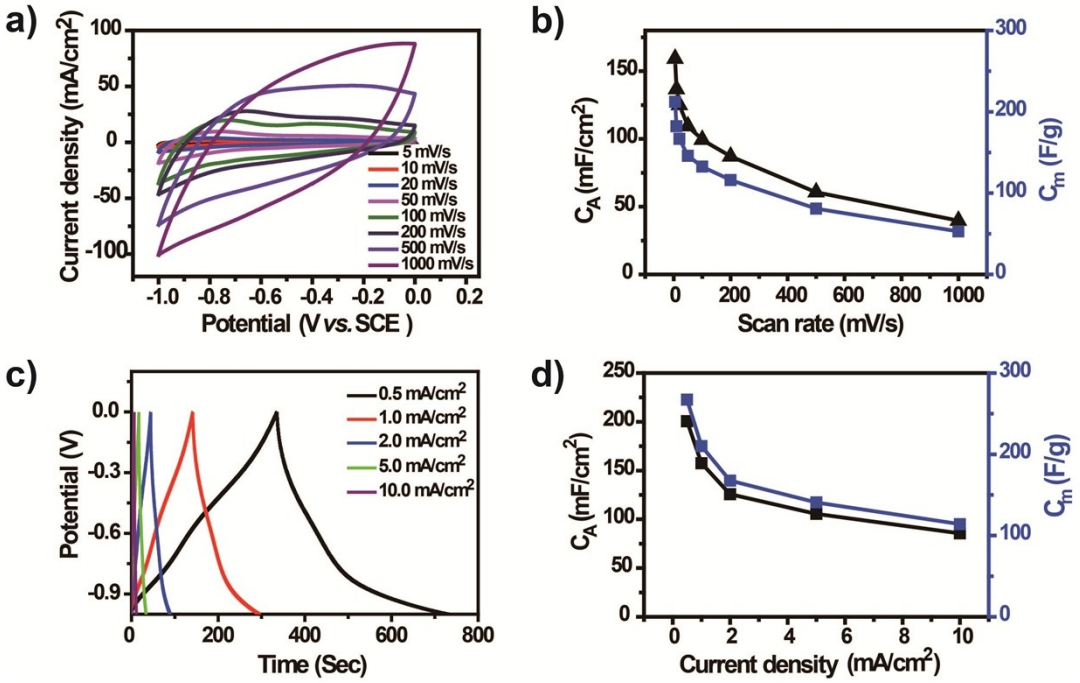

Fig. S4 Electrochemical performance of the 3D NF/rGO/H-Fe_2O_3 electrode. **a)** CV curves at different scan rates in 1.0 M Li_2SO_4 electrolyte; **b)** Areal- and mass-capacitance calculated from CV curves as a function of scan rates, respectively; **c)** Galvanostatic charge-discharge curves at different current densities; **d)** Areal- and mass-capacitance calculated from GCD curves as a function of current densities.

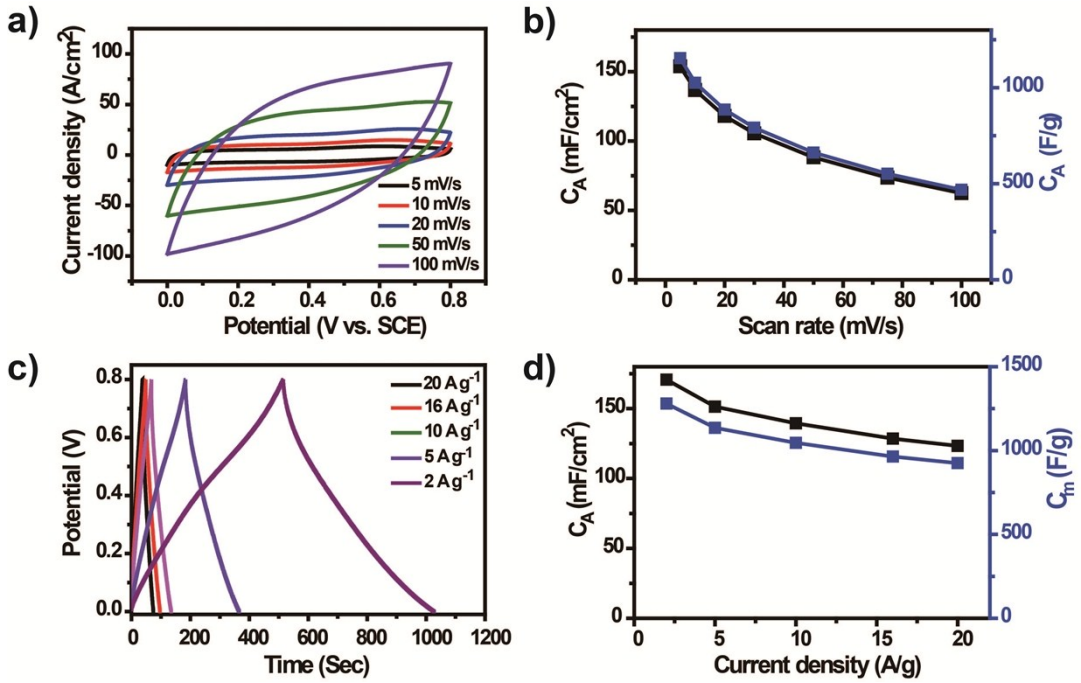

Fig. S5 Electrochemical performance of the 3D ZNs/ADM electrode. **a)** CV curves at different scan rates in 1.0 M Li_2SO_4 electrolyte; **b)** Areal- and mass-capacitance calculated from CV curves as a function of scan rates, respectively; **c)** Galvanostatic charge-discharge curves at different current densities; **d)** Areal- and mass-capacitance calculated from GCD curves as a function of current densities.

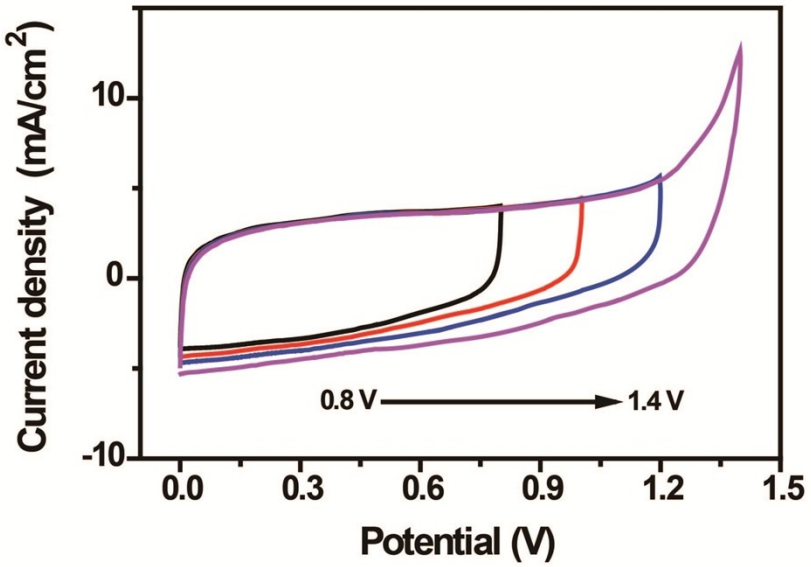

Fig. S6 CV curves for ZNs/ADM//NF/rGO/H-Fe_2O_3 asymmetric supercapacitor at different potential windows at scan rates of 1 V/s.

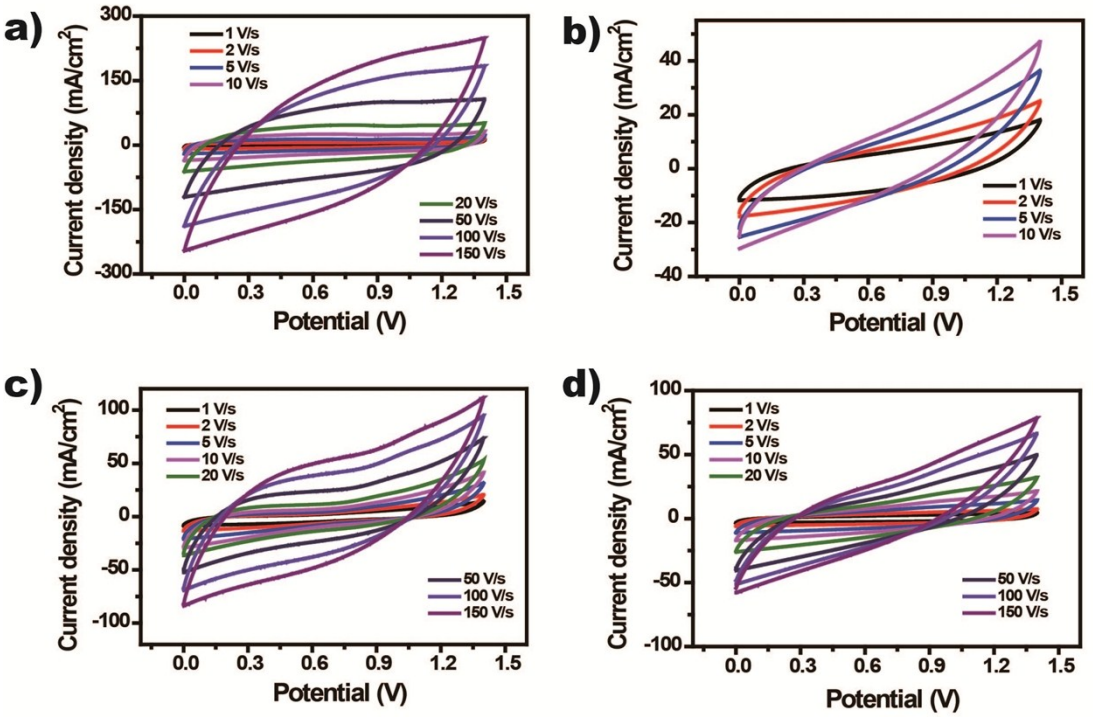

Fig. S7 Electrochemical characterization of asymmetric supercapacitors. CV curves for ZNs/ADM//NF/rGO/H-Fe_2O_3 (**a**), ZNs/ADM//NF/rGO/Fe_2O_3 (**b**), ZNs/ADM//NF/H-Fe_2O_3 (**c**), and ZNs/ADM//NF/rGO (**d**) asymmetric supercapacitors at scan rates from 1 to 10 or 150 V/s, respectively.

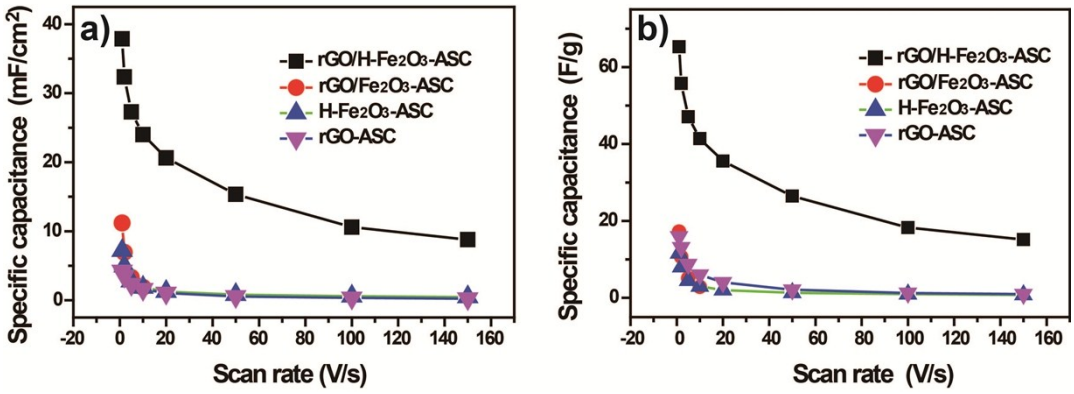

Fig. S8 Areal- (**a**) and mass-capacitance (**b**) of ZNs/ADM//NF/rGO/H-Fe_2O_3, ZNs/ADM//NF/rGO/Fe_2O_3, ZNs/ADM//NF/H-Fe_2O_3, and ZNs/ADM//NF/rGO ASCs calculated from CV curves as a function of scan rates.

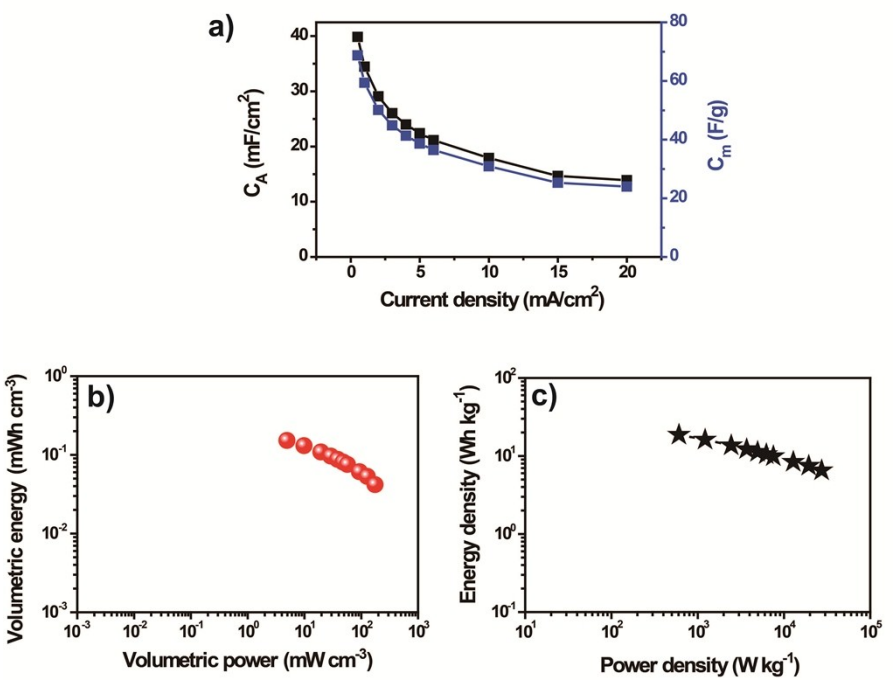

Fig. S9 a) Areal- and mass-capacitance of ZNs/ADM//NF/rGO/H-Fe_2O_3 calculated from the discharge curves as a function of current density; **b**) Volumetric energy and power densities of ZNs/ADM//NF/rGO/H-Fe_2O_3 calculated from GCD curves as a function of the current densities; **c**) Mass energy and power densities of ZNs/ADM//NF/rGO/H-Fe_2O_3 calculated from GCD curves as a function of the current densities.

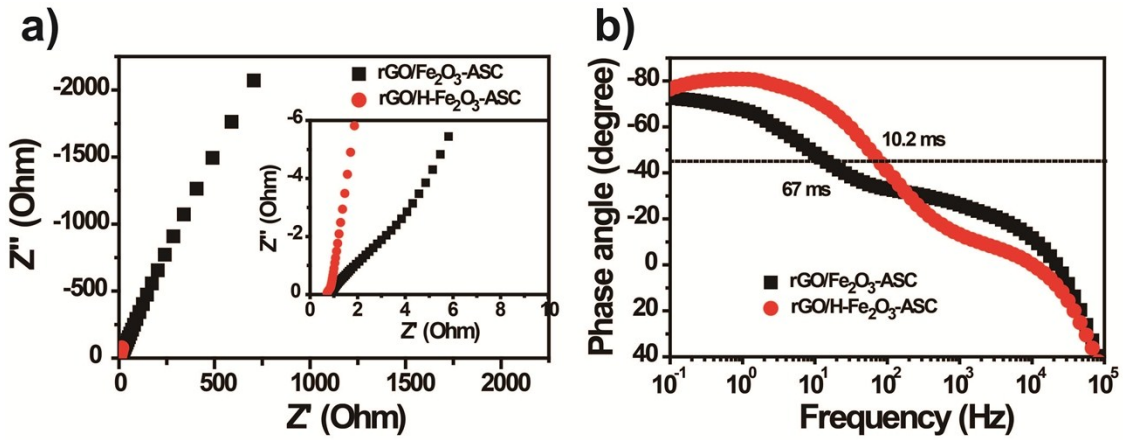

Fig. S10 a) Impedance spectra of the ZNs/ADM//NF/rGO/H-Fe_2O_3 and ZNs/ADM//NF/rGO/Fe_2O_3 ASCs, respectively. The inset shows an enlarged view of the impedance spectra in the high frequency region; **b)** The phase angle versus the frequency of the ZNs/ADM//NF/rGO/H-Fe_2O_3 and ZNs/ADM//NF/rGO/Fe_2O_3 ASCs, respectively.

Table S1. Comparison results on the basis of ZNs/ADM (positive)//rGO/H-Fe_2O_3 (negative) asymmetric supercapacitor and earlier reports.

Supercapacitors	Specific capacitance	Energy density (Max)	Power density (Max)	Ref.
ZNs/ADM//rGO/H-Fe_2O_3	37.88 mF/cm^2 (1 V/s) 65.31 F/g	0.14 mWh/cm^3	12.30 W/cm^3	This work
ZNs/ADM//rGO/Fe_2O_3	11.19 mF/cm^2 (1 V/s) 17.22 F/g	0.03 mWh/cm^3	0.13 W/cm^3	This work
ZNs/ADM//H-Fe_2O_3	7.18 mF/cm^2 (1 V/s) 11.59 F/g	0.02 mWh/cm^3	0.61 W/cm^3	This work
ZNs/ADM//rGO	4.25 mF/cm^2 (1 V/s) 15.95 F/g	0.01 mWh/cm^3	0.28 W/cm^3	This work
Ta_2O_5-NTs/C-Fe_2O_3-SC	4.6 mF/cm^2 (1 V/s)			[64]
LSG-EC	3.67 mF/cm^2 (1 A/g) 4.04 mF/cm^2 (1 A/g, in 1.0 M H_2SO_4)			[8]
EG/PH1000 MSC	5.40 mF/cm^2 (1 mV/s)			[11]
rGO-MSC	0.54 mF/cm^2 (500 mV/s)			[65]
MPG-MSC	80.7 μF/cm^2 (10 mV/s)			[14]
BNC/CNT-SC	18.8 mF/cm^2 (100 mV/s)			[Ref-S1]
LSG-EC		~0.07 mWh/cm^3	~2.1 W/cm^3	[8]
TiN-SC		~0.05 mWh/cm^3	~0.3 W/cm^3	[66]
3D-graphene-CNTs (Na_2SO_4)		~0.16 mWh/cm^3	~30 W/cm^3	[67]
H-ZnO@ZnO-doped MnO_2		~0.04 mWh/cm^3	~20 W/cm^3	[68]
SiC NW-SC		~0.007 mWh/cm^3	~5.95 W/cm^3	[24]
LSG-sandwich (PVA-H_2SO_4)		~0.105 mWh/cm^3	~6 W/cm^3	[13]
63V/220μF-EC		~0.07 mWh/cm^3	~300 W/cm^3	[19]
3V/300μF-Al EC		~0.001 mWh/cm^3	~48 W/cm^3	[19]
NDCNTs/ANPDM//Fe_2O_3-ASC		0.097 mWh/cm^3	28 mW/cm^3	[42]
HZM-SC		0.032 mWh/cm^3	~18 mW/cm^3	[68]
TiO_2@PPy-SC		0.013 mWh/cm^3	0.147 W/cm^3	[Ref-S2]
TiO_2@C-based-SCs		0.011 mWh/cm^3	0.032 W/cm^3	[Ref-S3]

References

[S1] Y. J. Kang, S.-J. Chun, S.-S. Lee, B.-Y. Kim, J. H. Kim, H. Chung, S.-Y. Lee, W. Kim, ACS Nano 2012, 6, 6400.
[S2] M. Yu, Y. Zeng, C. Zhang, X. Lu, C. Zeng, C. Yao, Y. Yang, Y. Tong, Nanoscale 2013, 5, 10806.
[S3] H. Zheng, T. Zhai, M. Yu, S. Xie, C. Liang, W. Zhao, S. C. I. Wang, Z. Zhang, X. J. Lu, Mater. Chem. C 2013, 1, 225.